Pointing out the Convolution Problem of Stochastic Aggregation Methods for the Determination of Flexibility Potentials at Vertical System Interconnections

Johannes Gerster
and Sebastian Lehnhoff
Department of Computing Science
CvO Universität Oldenburg
Email: johannes.gerster@uol.de

Marcel Sarstedt
and Lutz Hofmann
Institute of Electric Power Systems
Leibniz Universität Hannover
Email: sarstedt@ifes.uni-hannover.de

Eric MSP Veith
OFFIS e.V.
R&D Division Energy
Oldenburg, Germany
Email: eric.veith@offis.de

***Abstract*—The increase of generation capacity in the area of responsibility of the Distribution System Operator requires strengthening of coordination between Transmission System Operator and Distribution System Operator in order to prevent conflicting or counteracting use of flexibility options. For this purpose, methods for the standardized description and identification of the aggregated flexibility potential of distribution grids are developed in the context of Smart Grids management and control. Approaches for identifying the flexible operation region of distribution grids can be categorized into two main classes: Data-driven/stochastic approaches and optimization-based approaches. While the latter have the advantage of working in real-world scenarios where no full grid models exist, when relying on naïve sampling strategies, they suffer from poor coverage of the edges of the feasible operation region. To underpin the need for improved sampling strategies for data-driven approaches, in this paper we point out and analyse the shortcomings of naïve sampling strategies with focus on the problem of leptocurtic distribution of resulting interconnection power flows. We refer to this problem as *convolution problem*, as it can be traced back to the fact that the probability density function of the sum of two or more independent random variables is the convolution of their respective probability density functions. To demonstrate the *convolution problem*, we construct a series of synthetic 0.4 kV feeders, which are characterized by an increasing number of nodes and apply a sampling strategy to them that draws set-values for the controllable distributed energy resources from independent uniform distributions. By calculating the power flow for each sample in each feeder, we end up with a collapsing point cloud of interconnection power flows clearly indicating the *convolution problem*.**

Keywords*—*TSO/DSO-coordination; convolution of probability distributions; aggregation of flexibilities; feasible operation region; hierarchical grid control.

I. Introduction

The increasing share of Distributed Energy Resources (DERs) in the electrical energy system leads to new challenges for both, Transmission System Operator (TSO) and Distribution System Operator (DSO). Flexibility services for congestion management and balancing, so far mostly provided by large scale thermal power plants directly connected to the Transmission Grid (TG), increasingly have to be provided by DERs connected to the Distribution Grid (DG). Thus, DGs evolve from formerly mostly passive systems to Active Distribution Grids (ADGs) that contain a variety of controllable components interconnected via communication infrastructure and whose dynamic behaviour is characterized by higher variability of power flows and greater simultaneity factors.

TSO-DSO coordination is an important topic which has been pushed by ENTSO-E during the last years [1]–[4]. Coordination between grid operators has to be strengthened to prevent conflicting or counteracting use of flexibility options [5]. To reduce complexity for TSOs at the TSO/DSO interface and to enable TSOs to consider the flexibility potential of DGs in its operational management and optimization processes, methods are needed which allow for the determination and standardized representation of the aggregated flexibility potential of DGs.

The aggregated flexibility potential of a DG can be described as region in the PQ-plane that is made up from the set of feasible Interconnection Power Flows (IPFs) [6]. Thereby, feasible IPFs are IPFs which can be realized by using the flexibilities of controllable DERs and controllable grid components such as On-Load Tap Changer (OLTC) transformers in compliance with grid constraints i.e., voltage limits and maximum line currents.

In the literature, there are various concepts to determine the Feasible Operation Region (FOR) of DGs. They can be categorized into two main classes: Data-driven/stochastic approaches and optimization-based approaches.

For data-driven approaches, the general procedure is such that a set of random control scenarios is generated by assigning set-values from a uniform distribution to each controllable unit. By means of load flow calculations, the resulting IPFs are determined for each control scenario and classified into feasible IPFs (no grid constraints are violated) and non-feasible IPFs (at least one grid constraint is violated). The resulting point cloud of feasible IPFs in the PQ-plane serves as stencil for the FOR [6]. A problem that comes with this approach is that drawing set-values from independent uniform distributions leads to an unfavourable distribution of the resulting IPFs in the PQ-plane and extreme points on the margins of the FOR are not captured well [7].

This is where optimization-based methods come into play. The basic idea behind these methods is not to randomly sample IPFs but systematically identify marginal IPFs by solving a series of Optimal Power Flow (OPF) problems [8]. In addition to better coverage of the FOR, optimization-based approaches have the advantage of higher computational efficiency. An important drawback is however that, except

 ISBN: 978-1-61208-855-6

for approaches which solve the OPF heuristically, solving the underlying OPF requires an explicit grid model [9]. On the other hand, the only heuristic approach published so far, suffers from poor automatability as it relies on manual tweaking of hyperparameters [10].

In practice, considering the huge size of DGs, complete data related to grid topology (data related to operating equipment incl. its characteristics and topological connections) is not commonly stored [11], which complicates parametrization of explicit grid models. In such circumstances, black-box machine learning (ML) models trained on measurement data provided by current smart meters can be an alternative to physics-based, explicit grid models [12]. Due to their compatibility with black-box grid models, we argue that it is worthwhile to research and improve data-driven approaches to determine the FOR of DGs. This paper is intended to point out and analyse the problem of leptocurtic distribution of IPFs with naïve sampling strategies and thus to underpin the need for more effective and more efficient data-driven sampling strategies, such as those published by Contreras *et al.* [13], when this paper was already advanced.

The remainder of the paper is structured as follows: A survey on existing approaches (data-driven and optimization-based) and the contribution of this paper are given in Section II. Next, in Section III the construction of a series of synthetic feeders with increasing number of nodes is explained. On the basis of these feeders, we performed our sampling experiments, whose results are presented in Section IV. Finally, in Section V the paper is summarized, the conclusion is given and an idea for a distributed sampling strategy is presented which does not suffer from unfavourable distribution of resulting IPFs.

II. Survey on grid flexibility aggregation methods and contribution of this paper

As outlined in the introduction, relevant literature can be grouped into two main categories: Data-driven/stochastic and optimization-based approaches for exploring the FOR of DGs.

A. Data-driven approaches

Heleno *et al.* [7] are the first to come up with the idea of estimating the flexibility range in each primary substation node to inform the TSO about the technically feasible aggregated flexibility of DGs. In order to enable the TSO to perform a cost/benefit evaluation, they also include the costs associated with adjusting the originally planned operating point of flexible resources in their algorithm. In the paper two variants of a Monte Carlo simulation approach are presented, which differ in the assignment of set-values to the flexible resources. While in the first approach independent random set-values for changing active and reactive power injection are associated to each flexible resource, in the second approach a negative correlation of one between generation and load at the same bus was considered. In a direct comparison of the two presented approaches, the approach with negative correlation between generation and load at the same bus performs better and results in a wider flexibility range and lower flexibility costs with a smaller sample size. Nevertheless, even with this approach, the capability to find marginal points in the FOR is limited. Therefore, in the outlook the authors suggest the formulation of an optimization problem in order to overcome the limitations of the Monte Carlo simulation approach, increasing the capability to find extreme points of the FOR and reducing the computational effort. In Silva *et al.* [8], which is discussed in the next subsection, the authors take up this idea again.

Mayorga Gonzalez *et al.* [6] extend in their paper the methodology presented by Heleno *et al.* [7]. First, they describe an approach to approximate the FOR of an ADG for a particular point in time, assuming that all influencing factors are known. For this, they use the first approach of Heleno *et al.* [7] for sampling IPFs (the one that does not consider correlations). That is, random control scenarios are generated by assigning set-values from independent uniform distributions to all controllable units. In contrast to [7], no cost values are calculated for the resulting IPFs. Instead, for describing the numerically computed FOR with sparse data, the region is approximated with a polygon in the complex plane. In addition, a probabilistic approach to assess in advance the flexibility associated to an ADG that will be available in a future time interval under consideration of forecasts which are subject to uncertainty is proposed. The authors mention that for practical usage the computation time for both approaches has to be significantly reduced. However, the problem of unfavourable distribution of the resulting IPF point cloud, when drawing control scenarios from independent uniform distributions, which is a mayor factor for the low computational efficiency, is not discussed.

When this paper was already advanced, Contreras *et al.* [13] came up with new sampling methods for data-driven approaches. They show that, when focusing the vertices of the flexibility chart of flexibility providing units during sampling, the quality of the data-driven approach can be dramatically improved in comparison to the naïve sampling. On top of that, they present a comparison of OPF-based and data-driven approaches, whose results show that with their improved sampling strategies both approaches are capable of assessing the FOR of radial distribution grids. But for grids with large number of buses, OPF-based methods are still better suited.

B. Optimization-based approaches

Silva *et al.* [8] address the main limitation of their sampling-based approach in Heleno *et al.* [7], namely estimating extreme points in the FOR. To this end, they propose a methodology which is based on formulating an optimization problem with below-mentioned objective function, whose minimization for different ratios of α and β allows to capture the perimeter of the flexibility area.

$$\alpha\, P_{DSO \to TSO} + \beta\, Q_{DSO \to TSO} \tag{1}$$

where $P_{DSO \to TSO}$ and $Q_{DSO \to TSO}$ are the active and reactive power injections at the TSO-DSO boundary nodes. Silva *et al.* [8] work out that the underlying optimization

problem represents an OPF problem. Due to its robust characteristics, they use the primal-dual, a variant of the interior point methods to solve it. The methodology was evaluated in simulation and validated in real field-tests on MV distribution networks in France. The comparison of simulation results with the random sampling algorithm in Heleno *et al.* [7] shows the superiority of the optimization-based approach by illustrating its capability to identify a larger flexibility area and to do it within a shorter computing time.

Capitanescu [14] proposes the concept of active-reactive power (PQ) chart, which characterizes the short-term flexibility capability of active distribution networks to provide ancillary services to TSO. To support this concept, an AC optimal power flow-based methodology to generate PQ capability charts of desired granularity is proposed and illustrated in a modified 34-bus distribution grid.

Contreras *et al.* [9] present a linear optimization model for the aggregation of active and reactive power flexibility of distribution grids at a TSO-DSO interconnection point. The power flow equations are linearized by using the Jacobian matrix of the Newton-Raphson algorithm. The model is complemented with non-rectangular linear representations of typical flexibility providing units, increasing the accuracy of the distribution grid aggregation. The obtained linear programming system allows a considerable reduction of the required computing time for the process. At the same time, it maintains the accuracy of the power flow calculations and increases the stability of the search algorithm while considering large grid models.

Fortenbacher *et al.* [15] present a method to compute reduced and aggregated distribution grid representations that provide an interface in the form of active and reactive power (PQ) capability areas to improve TSO-DSO interactions. Based on a lossless linear power flow approximation, they derive polyhedral sets to determine a reduced PQ operating region capturing all voltage magnitude and branch power flow constraints of the DG. While approximation errors are reasonable, especially for low voltage grids, computational complexity is significantly reduced with this method.

Sarstedt *et al.* [10] provide a detailed survey on stochastic and optimization based methods for the determination of the FOR. They come up with a comparison of different FOR determination methods with regard to quality of results and computation time. For their comparison, they use the Cigré medium voltage test system. On top of that, they present a Particle Swarm Optimization (PSO) based method for FOR determination.

Contributions of this paper

In summary, it can be stated that optimization-based approaches show high computational efficiency with good coverage of the FOR. However, methods used for solving the underlying OPF problem rely—except for heuristic approaches, which have other drawbacks—on explicit grid models of the DG, which must be parametrized with grid topology data often not available in practice. Data-driven approaches, on the other hand, do not require explicit grid modeling and are compatible with black-box grid models, but suffer from low computational efficiency and poor coverage of peripheral regions of the FOR, when using conventional sampling strategies.

This is where our approach comes in. We are heading towards improved sampling strategies for data-driven approaches, which mitigate the weak points of data-driven methods (low computational efficiency and poor coverage of FOR) while retaining their advantage of being compatible with black-box grid models. As a basis for this, in this paper we are the first to come up with an experiment setup by means of which the problem of resulting convoluted distribution of IPFs with naïve sampling strategies can be analyzed and pointed out in an easily reproducible manner.

III. Experiment setup

To show the shortcomings of naïve sampling strategies, we apply a sampling strategy that draws set-values for the controllable DERs from indpendent uniform distributions to a series of synthetic $0.4\,\mathrm{kV}$ feeders as shown in Figure 1. The feeders are characterized by an increasing number of nodes. To be able to consider the effect of the number of nodes on the IPF-sample as isolated as possible, both, the total installed power and the average transformer-node distance are chosen equal for all feeders. The installed power is distributed equally among all connected DERs:

$$P^i_{inst,DER_j} = \frac{P^i_{inst,DERs}}{N^i}, \tag{2}$$

where P^i_{inst,DER_j} is the installed power of the DER connected to the jth node n^i_j of feeder i, $P^i_{inst,DERs}$ is the total installed power of feeder i and N^i is the number of nodes of feeder i. Nodes are equally distributed along feeders as shown in Figure 1 and the line length between adjacent nodes l^i_l of feeder i with length l^i_f is:

$$l^i_l = \frac{l^i_f}{N^i}. \tag{3}$$

The transformer-node distance of node n^i_j is:

$$d^i_{t,n_j} = l^i_l \cdot j. \tag{4}$$

With (4) the average transformer-node distance $\overline{d^i_{t,n}}$ of feeder i can be written as:

$$\begin{aligned} \overline{d^i_{t,n}} &= \frac{1}{N^i}\sum_{j=1}^{N^i} d^i_{t,n_j} \\ &= \frac{1}{N^i}\sum_{j=1}^{N^i} l^i_l \cdot j = \frac{l^i_l}{N^i}\sum_{j=1}^{N^i} j \\ &= \frac{l^i_l}{N^i}\cdot\frac{N^i_j\cdot(N^i_j+1)}{2}. \end{aligned} \tag{5}$$

Resolved after the line length l^i_l, the result is:

$$l^i_l = \overline{d^i_{t,n}}\cdot\frac{2}{N^i+1}. \tag{6}$$

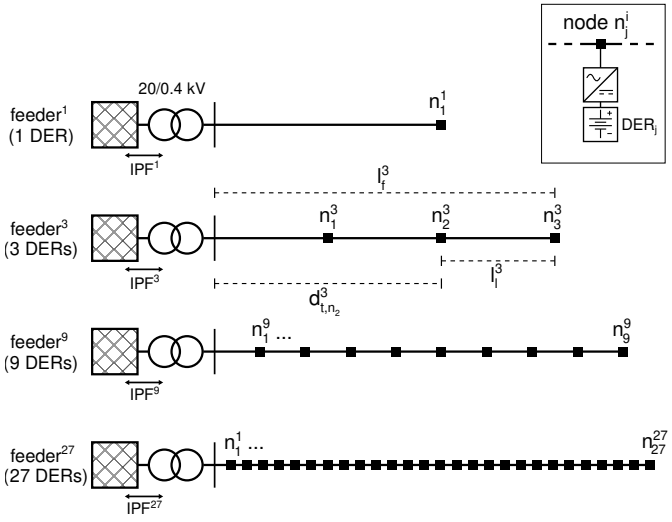

Figure 1. Synthetic 0.4 kV feeders

With (3) and (6) the length of feeder i results in:

$$l_f^i = \overline{d_{t,n}^i} \cdot \frac{2N^i}{N^i + 1}. \tag{7}$$

For our experiments, we have constructed four synthetic 0.4 kV feeders. The feeders differ in the number of nodes N^i, which has been set to 1, 3, 9 or 27, respectively. Line length l_l^i and feeder length l_f^i have then been calculated according to (6) and (7). There is one DER connected to each node and the installed power $P^i_{inst,DERs}$ is distributed evenly among the DERs according to (2). To be able to cover the entire flexibility area of the feeders including its border areas where voltage band violations and/or line overloadings can be observed, all DERs are inverter-connected battery storages because they offer maximum flexibility with regard to both, active and reactive power provision. The dimensioning of the inverters has been chosen in such a way that a power factor $\cos\phi$ of 0.9 can be kept, when the maximum active power is delivered:

$$|S|^i_{max,DER_j} = \frac{P^i_{inst,DER_j}}{\cos\phi} = \frac{P^i_{inst,DER_j}}{0.9}. \tag{8}$$

Active and reactive power ranges of the battery storages are thus:

$$\begin{aligned}\left[P^i_{min,DER_j}, P^i_{max,DER_j}\right] &= \left[-P^i_{inst,DER_j}, P^i_{inst,DER_j}\right] \\ \left[Q^i_{min,DER_j}, Q^i_{max,DER_j}\right] &= \left[-|S|^i_{max,DER_j}, |S|^i_{max,DER_j}\right].\end{aligned} \tag{9}$$

Values for the technical parameters of the four feeders including connected DERs are listed in Table I.

For all feeders, we conduct the sampling in such a way that for each DER and each sample element we independently draw real and reactive power values from uniform distributions:

$$\begin{aligned}\mathcal{X}^i_{P,DER_j} &\sim \mathcal{U}^i_j\left[P^i_{min,DER_j}, P^i_{max,DER_j}\right] \\ \mathcal{X}^i_{Q,DER_j} &\sim \mathcal{U}^i_j\left[Q^i_{min,DER_j}, Q^i_{max,DER_j}\right].\end{aligned} \tag{10}$$

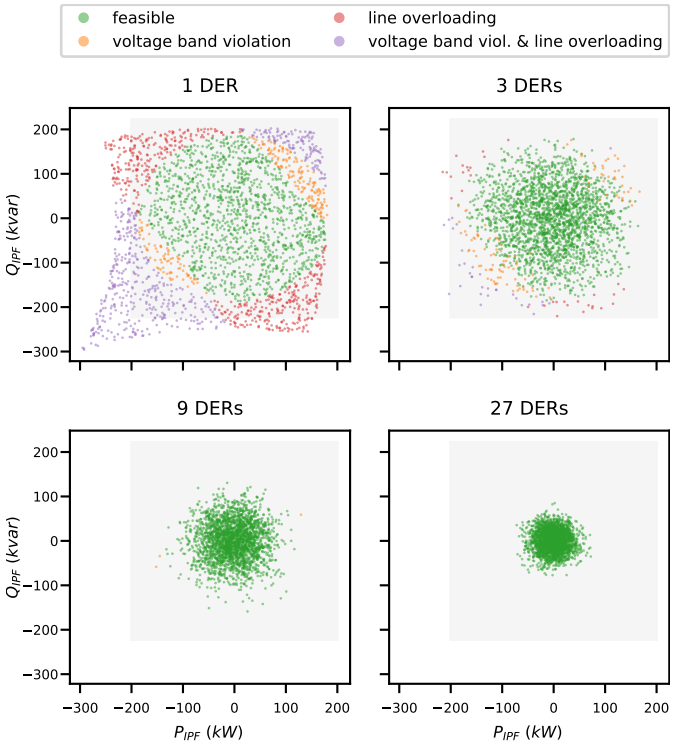

Figure 2. Results of naïve sampling strategy classified by feasibility with regard to grid constraints (voltage band limits and max. line loading); inverter constraints are neglected

After assigning active and reactive power values to each DER, the *pandapower* library [16] calculates the power flow. This way we generate a sample of size 2500 for each feeder.

Following this, the sample elements are first classified with regard to their adherence to grid constraints and in case of non-adherence with regard to the type of grid constraint violation (i.e., voltage band violation, line overload, or both). Second, inverter constraints are taken into account and the sample elements are classified with regard to adherence to both, grid and inverter constraints. In this case, sample elements are only classified as feasible, if neither grid constraints nor device constraints for any of the connected inverters occur. In case of non-feasibility, we distinguish depending on the type of constraint violation (i.e., grid constraint violation, inverter constraint violation, or both).

Finally, we plot the classification results in the domain of active and reactive IPFs P_{IPF} and Q_{IPF}.

IV. Experiment Results

The resulting plots are shown in Figure 2 and 3. The sampling has been performed once for each feeder from Figure 1. This means that Figure 2 and 3 only differ in how the sample elements are classified. While for Figure 2 only grid constraints have been considered, Figure 3 also incorporates inverter constraints. Both figures consist of four subplots—one for each of the four feeders from Figure 1. Each dot of the point clouds represents one sample element—so every subplot contains 2500

 ISBN: 978-1-61208-855-6

TABLE I. CONFIGURATION OF THE SYNTHETIC FEEDERS

# DERs	P_{inst,DER_j} (kW)	$\|S\|_{max,DER_j}$ (kVA)	Feeder Length (m)	Line Length (m)	Line Type	Voltage Band (pu)	Trafo Type
1	200.0	222.2	400	400	NAYY 4x150 SE	0.9–1.1	0.4 MVA 20/0.4 kV
3	66.7	74.1	600	200	NAYY 4x150 SE	0.9–1.1	0.4 MVA 20/0.4 kV
9	22.2	24.7	720	80	NAYY 4x150 SE	0.9–1.1	0.4 MVA 20/0.4 kV
27	7.4	8.2	771	29	NAYY 4x150 SE	0.9–1.1	0.4 MVA 20/0.4 kV

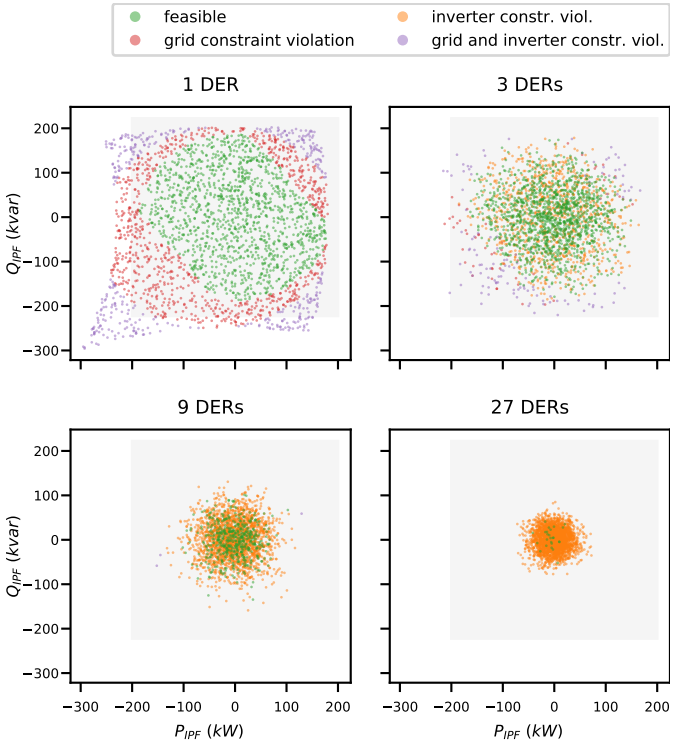

Figure 3. Results of naïve sampling strategy classified by feasibility with regard to both, grid and inverter constraints; please note: green dots are plotted above orange dots, i.e., no green dots are covered by orange dots

dots. The shaded grey area marks the theoretically known aggregated power limit for the DERs:

$$\begin{aligned}\left[P^i_{min,DERs}, P^i_{max,DERs}\right] &= \left[-P^i_{inst,DERs}, P^i_{inst,DERs}\right] \\ \left[Q^i_{min,DERs}, Q^i_{max,DERs}\right] &= \left[-|S|^i_{max,DERs}, |S|^i_{max,DERs}\right] .\end{aligned} \tag{11}$$

For the 1 DER case, shape and structure of the point cloud look as one would expect from the configuration. It largely covers the grey area—only slightly skewed and shifted towards lower active and reactive power values, which results from active and reactive power consumption of grid elements (lines and transformer). However, when increasing the number of DERs, the *convolution problem* becomes obvious. With 3 DERs, the feasible area is still covered to some extent, but the point density already decreases strongly towards the edges. In case of 9 DERs, the point density in the edges has decreased to such an extent that hardly any sample elements are detected which show grid constraint violations. Finally, with 27 DERs the point cloud has collapsed to a fraction of the grey area and only a small part of the theoretical FOR is covered.

From the 3 DERs subplot in Figure 2, it can be seen that with increasing number of DERs not only the region covered by the sample collapses, but at the same time the border between feasible and infeasible elements (with regard to grid constraints) becomes less distinct: The absence of a sharp border between feasible and non-feasible IPFs complicates the use of multi-class classification for identifying the FOR from the sample and indicates the use of a one-class classifier for that purpose.

Figure 3, which additionally considers inverter constraints, shows an other problem of the naïve sampling approach: In this consideration, not only the total area covered by the sample decreases, but also the share of feasible examples shrinks sharply, such that with 27 DERs only very few sample elements are identified which violate neither grid nor inverter constraints.

This is because with the naïve sampling approach power values are assigned to each DER at once. After that, the power flow calculation is performed and only at the very end the feasiblity with regard to grid and inverter constraints is checked. Even if the constraints of only a single inverter are violated, the example is classified as non-feasible with regard to inverter constraints. If, for example, for a single converter one third of the possible power setpoints violate constraints, the likelihood to observe no constraint violations with N inverters amounts to

$$\left(1 - \frac{1}{3}\right)^N .$$

For $N = 27$ inverters this would amount to approximately 1.76×10^{-5}.

One way to address this would be to perform a successive sampling as proposed by Bremer *et al.* [17] for the use case of active power planning. With successive sampling the evaluation of inverter constraints is done immediately after the assignment of setpoints to single DERs and in case of non-feasibility drawing of setpoints is repeated until a valid configuration is found. The power flow calculation would then be carried out only after setpoints compatible with inverter constraints have been found for each DER.

To illustrate the *convolution problem*, in Figure 4 we plot the frequency density of active IPFs resulting from our sampling against the Probability Density Function (PDF) of the Bates distribution. The Bates distribution is the continuous probability distribution of the mean of n independent uniformly distributed

 ISBN: 978-1-61208-855-6

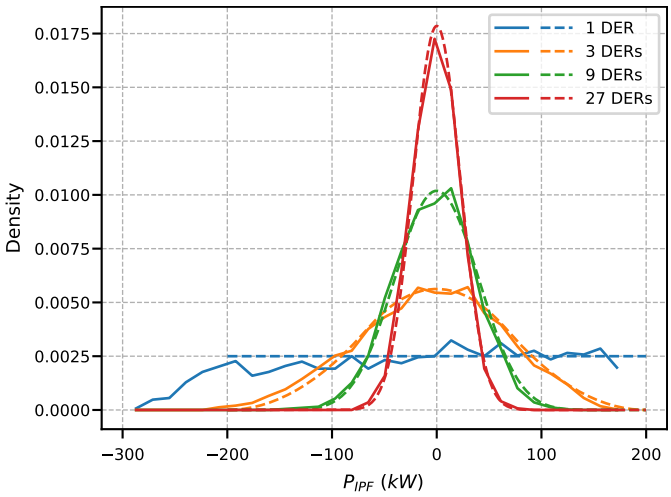

Figure 4. Frequency density of active IPFs resulting from our experiments (solid lines) compared with probability density function of Bates distribution on the interval $[-P^i_{inst,DERs}, P^i_{inst,DERs}]$ (dashed lines)

random variables on the unit interval and thus closely related to the Irwin-Hall distribution, which describes the sum of n independent uniformly distributed random variables. More general, in statistics the probability distribution of the sum of two or more independent random variables is the convolution of their individual distributions. For the variant of the Bates distribution generalized to arbitrary intervals $[a, b]$:

$$\mathcal{X}_{(a,b)} = \frac{1}{n}\sum_{k=1}^{n}\mathcal{U}_k(a,b) \tag{12}$$

this results in the following equation defining the PDF:

$$f(x) = \begin{cases} \sum_{k=0}^{n}\left[(-1)^k\binom{n}{k}\left(\frac{x-a}{b-a}-\frac{k}{n}\right)^{n-1} \right. & \text{if } x \in [a,b] \\ \left. \quad \operatorname{sgn}\left(\frac{x-a}{b-a}-\frac{k}{n}\right)\right] & \\ 0 & \text{otherwise.} \end{cases} \tag{13}$$

Comparison with the Bates distribution is motivated by the fact that with equations (2), (9) and (10) the active power range from which we draw values during the sampling can be written as follows:

$$\begin{aligned} \mathcal{X}^i_{P,DER_j} &\sim \mathcal{U}^i_j\left[\frac{-P^i_{inst,DERs}}{N^i}, \frac{P^i_{inst,DERs}}{N^i}\right] \\ &= \frac{1}{N^i}\mathcal{U}^i_j\left[-P^i_{inst,DERs}, P^i_{inst,DERs}\right]. \end{aligned} \tag{14}$$

For a single sample element the active IPF P^i_{IPF} is made up of the sum of active power injections of connected DERs $P^i_{DER_j}$ and the grid losses P^i_{loss}:

$$P^i_{IPF} = \sum_{j=1}^{N_i} P^i_{DER_j} + P^i_{loss} \tag{15}$$

We are interested in the distribution $\mathcal{X}^i_{P,IPF}$ of active IPFs. Ignoring grid losses P^i_{loss} in (15), with equations (14) and (15) we can write:

$$\begin{aligned} \mathcal{X}^i_{P,IPF} &\sim \sum_{j=1}^{N_i}\frac{1}{N^i}\mathcal{U}^i_j\left[-P^i_{inst,DERs}, P^i_{inst,DERs}\right] \\ &= \frac{1}{N^i}\sum_{j=1}^{N_i}\mathcal{U}^i_j\left[-P^i_{inst,DERs}, P^i_{inst,DERs}\right], \end{aligned} \tag{16}$$

which is exactly the Bates distribution on the interval $\left[-P^i_{inst,DERs}, P^i_{inst,DERs}\right]$.

V. Conclusion and Future Work

Aggregating the flexibility potential of DGs is an important prerequisite for effective TSO-DSO coordination in electric power systems with high share of generation located in the DG level. In this paper, we first gave an overview of existing flexibility aggregation methods and categorized them in terms of whether they are data-driven/stochastic or optimization-based. Following this, we discussed the strengths and weaknesses of both approaches (stochastic and optimization-based) and motivated the investigation of improved sampling strategies for data-driven approaches. As a basis for this, we presented an experimental setup by means of which we demonstrated and analyzed the shortcomings of naïve sampling strategies with focus on the problem of resulting leptokurtic distribution of IPFs.

In future work we will investigate approaches for mitigating the *convolution problem*. One idea is to formulate the sampling as a distributed optimization problem whose objective function takes into account the uniformity of the resulting set of IPFs. First experiments in this direction with the Combinatorial Optimization Heuristic for Distributed Agents (COHDA) protocol by Hinrichs *et al.* [18] and with Ripleys-K as metric for the evaluation of the distribution show promising results.

Additionally, we are working on making OPF-based methods compatible with black-box grid models by solving the underlying OPF with the help of evolutionary algorithms such as the covariance matrix adaptation evolution strategy (CMA-ES) [19] or REvol, an algorithm which was originally developed for training artificial neural networks [20]. Furthermore, we want to investigate if the total number of required objective function evaluations can be reduced when sampling the border of the FOR in one run by dynamically adapting the underlying objective function.

Acknowledgements

This work was funded by the Deutsche Forschungsgemeinschaft (DFG, German Research Foundation) – 359921210.

References

[1] ENTSO-E, “General guidelines for reinforcing the cooperation between TSO and DSO,” Tech. Rep., 2015.

[2] ——, “Towards smarter grids: Developing TSO and DSO roles and interactions for the benefit of consumers,” Position Paper, 2015.

[3] ——, “Distributed flexibility and the value of TSO/DSO cooperation – Fostering active customer participation to value their services on the market – An ENTSO-E position,” Policy Paper, Dec. 2017.

 ISBN: 978-1-61208-855-6

[4] ——, "TSO-DSO Report – An integrated approach to active system management with the focus on TSO-DSO coordination in congestion management and balancing," Tech. Rep., 2019.

[5] M. Sarstedt *et al.*, "Standardized evaluation of multi-level grid control strategies for future converter-dominated electric energy systems," *at - Automatisierungstechnik*, vol. 67, no. 11, pp. 936–957, Nov. 2019.

[6] D. Mayorga Gonzalez *et al.*, "Determination of the time-dependent flexibility of active distribution networks to control their TSO-DSO interconnection power flow," in *2018 Power Systems Computation Conference (PSCC)*. Dublin, Ireland: IEEE, Jun. 2018, pp. 1–8.

[7] M. Heleno *et al.*, "Estimation of the flexibility range in the transmission-distribution boundary," in *2015 IEEE Eindhoven PowerTech*. Eindhoven, Netherlands: IEEE, Jun. 2015, pp. 1–6.

[8] J. Silva *et al.*, "Estimating the active and reactive power flexibility area at the TSO-DSO interface," *IEEE Transactions on Power Systems*, vol. 33, no. 5, pp. 4741–4750, Sep. 2018.

[9] D. A. Contreras and K. Rudion, "Improved assessment of the flexibility range of distribution grids using linear optimization," in *2018 Power Systems Computation Conference (PSCC)*. Dublin, Ireland: IEEE, Jun. 2018, pp. 1–7.

[10] M. Sarstedt, L. Kluß, J. Gerster, T. Meldau, and L. Hofmann, "Survey and comparison of optimization-based aggregation methods for the determination of the flexibility potentials at vertical system interconnections," *Energies*, vol. 14, no. 3, p. 687, 2021.

[11] R. Singh, E. Manitsas, B. C. Pal, and G. Strbac, "A recursive Bayesian approach for identification of network configuration changes in distribution system state estimation," *IEEE Transactions on Power Systems*, vol. 25, no. 3, pp. 1329–1336, Aug. 2010.

[12] P. Barbeiro, J. Krstulovic, F. J. Soares, H. Teixeira, and J. P. Iria, "State estimation in distribution smart grids using autoencoders," *IEEE 8th International Power Engineering and Optimization Conference (PEOCO2014)*, pp. 358–363, 2014.

[13] D. A. Contreras and K. Rudion, "Computing the feasible operating region of active distribution networks: Comparison and validation of random sampling and optimal power flow based methods," *IET Generation, Transmission & Distribution*, vol. 2021, pp. 1–13, 2021.

[14] F. Capitanescu, "TSO–DSO interaction: Active distribution network power chart for TSO ancillary services provision," *Electric Power Systems Research*, vol. 163, pp. 226–230, Oct. 2018.

[15] P. Fortenbacher and T. Demiray, "Reduced and aggregated distribution grid representations approximated by polyhedral sets," *International Journal of Electrical Power & Energy Systems*, vol. 117, 2020, 105668.

[16] L. Thurner *et al.*, "Pandapower—An open-source Python tool for convenient modeling, analysis, and optimization of electric power systems," *IEEE Transactions on Power Systems*, vol. 33, no. 6, pp. 6510–6521, Nov. 2018.

[17] J. Bremer and M. Sonnenschein, "Sampling the search space of energy resources for self-organized, agent-based planning of active power provision," in *Environmental Informatics and Renewable Energies - 27th International Conference on Informatics for Environmental Protection*, Hamburg, Sep. 2013, pp. 214–222.

[18] C. Hinrichs and M. Sonnenschein, "A distributed combinatorial optimisation heuristic for the scheduling of energy resources represented by self-interested agents," *Int. J. of Bio-Inspired Computation*, vol. 10, no. 2, pp. 69–78, Jul. 2017.

[19] N. Hansen, "The CMA Evolution Strategy: A Comparing Review," *Towards a new evolutionary computation*, pp. 75–102, 2006.

[20] E. M. Veith, B. Steinbach, and M. Ruppert, "An evolutionary training algorithm for artificial neural networks with dynamic offspring spread and implicit gradient information," in *The Sixth International Conference on Emerging Network Intelligence (EMERGING 2014)*, Rome, Aug. 2014.

 ISBN: 978-1-61208-855-6